An Empirical Study on the Performance of Overshot Water Wheel in Very Low-Head Water Resources

Mohd Farriz Basar*‡, Izzatie Akmal Zulkarnain*, Kamaruzzaman Sopian**

* Fakulti Teknologi dan Kejuruteraan Elektrik (FTKE), Universiti Teknikal Malaysia Melaka (UTeM), Hang Tuah Jaya, 76100 Durian Tunggal, Melaka, Malaysia.

** Department of Mechanical Engineering, Universiti Teknologi PETRONAS, 32610 Seri Iskandar, Perak, Malaysia

(mfarriz@utem.edu.my, izzatieakmal@gmail.com, ksopian@utp.edu.my)

‡ Corresponding Author; Mohd Farriz Basar, FTKE, UTeM, 76100 Durian Tunggal, Melaka, Malaysia, Tel: +606 2704021, Fax: +606 2701052, mfarriz@utem.edu.my

Received: 14.12.2023 Accepted:23.01.2024

Abstract- The overshot water wheel is a common type of gravity turbine widely used in low-head and low-flow water applications. The primary objective of this study is to develop a simple overshot water wheel, referred to as the Bottle-Blade Overshot Water Wheel (BOWW), and to evaluate its efficiency while investigating the effects of varying water head levels and blade numbers. The BOWW utilises polyethylene bottles for blade fabrication, offering an innovative and environmentally friendly alternative to conventional water wheel designs. Experimental testing was conducted using a water test rig that simulates actual hydropower site conditions. Key performance parameters, including power output, rotational speed, torque, and system efficiency, were evaluated. The experimental performance of the BOWW was analysed using governing equations and compared with previously published results for breastshot and overshot water wheel turbines. The results show that the BOWW equipped with eight blades and operating at a 0.5 m head produced mechanical and electrical power outputs of 48.58 W and 15.55 W, respectively. The eight-blade configuration achieved an efficiency ranging from 26.8% to 49.1%, whereas the four-blade configuration exhibited efficiencies between 5.66% and 28.96%. The higher performance of the eight-blade BOWW is attributed to increased rotational speed, resulting in greater power output and efficiency. Overall, the findings demonstrate that the eight-blade BOWW is an effective and low-cost solution for low-head and low-flow hydropower applications.

Keywords Low head, low flow, overshot water wheel, pico hydropower.

1. Introduction

Electricity is crucial for fundamental activities such as cooling, lighting, and powering household appliances, making it a critical component for human development [1, 2, 3]. However, a significant portion of the population, particularly in underdeveloped rural areas, still lacks access to electricity [4]. Consequently, many off-grid communities rely on fossil fuel generators for their domestic electrical needs [5, 6, 7, 8]. Therefore, it is essential to explore sites with low water head resources (less than 10 m) for potential energy sources, as many villages are situated near rivers [3, 9, 10]

Gravity turbines, like the slow-running machine, operate at low water heads, typically less than 10 meters, and with a low water flow rate. Examples of such turbines include the Archimedes Screw, breastshot water wheel, pitchback water wheel, and overshot water wheel are the products of gravity turbines that perform effectively under low water head conditions [11, 12, 13 ,14].

A well-designed overshot water wheel turbine can achieve an impressive 85% efficiency with flow rates ranging from less than 0.01 to 0.1 m^3/s and water heads ranging from a few meters to ten meters [15, 16, 17]. The overshot water wheel is renowned as one of the most popular types of gravity turbines, particularly in low head and low flow conditions [9, 18, 19]. Its reputation is based on its high efficiency, even in situations with limited head and flow. Its design allows for effective operation at low head heights, and its simplicity makes it easier to construct and maintain, especially in off-grid locations [20, 21].

Furthermore, the overshot water wheel has come a long way in terms of efficiency since its initial testing by the British engineer John Smeaton in 1759, when it achieved an efficiency of over 60%, compared to 30% for the undershot water wheel [22]. Over time, advancements in materials, design structures, and operating principles have significantly improved its efficiency.

Nowadays, people began to innovate the turbine blades or water wheel bucket parts with recyclable alternatives, including empty polythene bottles, plastic bowls, coconut shells and large shells [23, 24]. These diversity of water turbines signifies that people have shown interest in developing sustainable water wheel designs.

This project employs the polythene bottles as turbine blades to replace the conventional use of zinc or wood in traditional water wheel. Such materials are not only expensive, but it also is prone to deterioration when exposed to moisture, such as corrosion and rot. The polythene bottle, on the other hand, is much cheaper and takes a vey long time to completely decompose, approximately 70 to 1000 years depending on the structure of material and environmental conditions [25]. In addition, this stand-alone hydropower generation system is considered to operate successfully for a minimum of two years without requiring major maintenance.

The objective of this research is to investigate the performance of BOWW (bottle-blade overshot water wheel), designed with a noncomplex geometric configuration using locally available materials that are readily accessible in local hardware stores. By utilizing locally available materials that are easily accessible, this project not only promotes sustainability but also empowers local communities. It does not only simplify the construction process but also encourages the community members to actively participate in renewable energy initiatives.

In testing the prototype within a laboratory setting, the research aims to validate not only the technical viability of the design but also its potential for practical implementation in real-world, community-based settings.

Three previous studies including undershot, breastshot and overshot water wheel turbines were used as primary sources of references for this research. The previous undershot water wheel comprised of twelve steel blades achieved an efficiency of 24% efficiency. Morever, the water wheel itself required skilful manpower to install the system due to its complex geometrical design, with a size of 2m length and 0.4m width [26].

İn contrast to undershot, the breastshot water wheel is equipped with sixteen steel blades and achieved 45% efficiency, with similar dimensions with undershot water wheel, 2m x 0.4m [27]. In another research of overshot water wheel, the turbine itself achieved good effeciency at 59%, however failed to operate effectively under 1m of water head [28].

2. Water Wheel Design

In this research, we introduce an overshot water wheel, referred as the bottle blades overshot water wheel (BOWW). The overall geometric design of the BOWW closely resembles that of traditional overshot water wheels, with significant modifications made to the blade components. While conventional overshot water wheels typically employ materials like steel and wood for crafting the blade components [8], the BOWW turbine takes an innovative approach by using plastic soda bottles with a capacity of 1.5liters as an alternative material for constructing the turbine blades, as illustrated in Fig. 1.

Fig. 1. Blade parts of BOWW.

Plastic soda bottles are employed as blades in their original, uncut shape to maximize their surface area. As depicted in Figure 1, three bottles are joined together using 12-inch (4.8x300mm) nylon cable ties before being attached to a 0.5-meter length of 1½-inch PVC pipe. Subsequently, PVC solvent cement is used to connect the pipe to the PVC male connector fittings, which serve as the blade holders. This process is repeated until a total of eight blades are created using 24 soda bottles, as illustrated in Fig. 2.

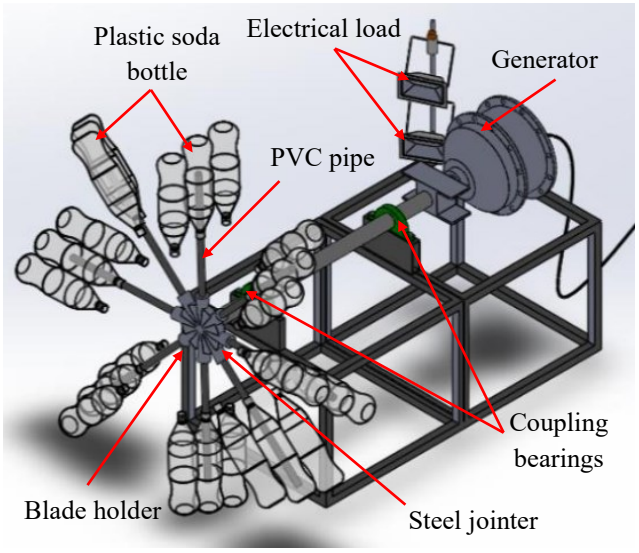

Fig. 2. Overshot water wheel using plastic bottles as blades.

Typically, the blades or buckets of a traditional overshot water wheel are made from materials such as wood or zinc

[29]. Conversely, as illustrated in Fig. 2, the BOWW system introduced a novel approach by utilizing turbine blade parts constructed from plastic soda bottles. These blades are mounted tangentially to the wheel and are designed to capture the water as it flows from the top of the wheel [11].

In contrast, as depicted in Fig. 2, this project introduces an innovative approach by utilizing plastic soda bottles to create the turbine's blade components. Among various types of plastic bottles, the 1.5liters soda bottles were selected for this purpose. Fig. 3 illustrates the components used and the final development of the BOWW turbine.

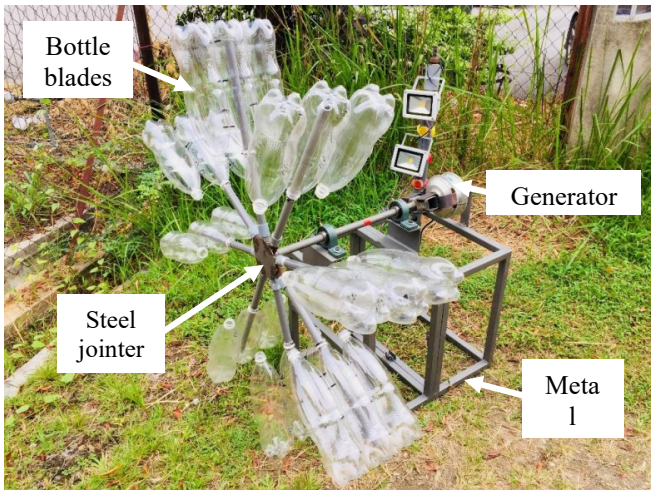

Fig. 3. Final development of BOWW turbine.

The components utilized for the turbine's development are listed below;

- 24 units of recyclable soda bottles
- 8 units of blades holder made of PVC male threaded adapter fittings with 0.5m length of 1½ inch PVC pipes
- 8 units of stainless-steel end caps
- 1 unit of stainless-steel round shaped surface

3. Experimental Test Rig

This research has made a significant contribution by designing a more effective and efficient experimental setup that is both straightforward to construct and closely replicates real-world scenarios in hydroelectric power plants. Additionally, the test rig harnesses the gravitational potential energy of the water tank, enabling it to generate a range of water heads from 0.3m to 0.5m and flow rates from 0.012m^3/s to 0.021m^3/s. This versatility makes the experimental setup suitable for both run-of-river and run-on-river techniques.

As depicted in Fig. 4, the water test rig comprises with proposed BOWW turbine, Prony brake system, water tank 1, water tank 2 and water pump. The water pump is utilized to transfer water from water tank 2 to water tank 1 via the water inlet and outlet. Subsequently, the water flows from water tank 1 into the open downstream water channel, simultaneously cascading onto the water wheel blades. Upon impact with the turbine's blades, the turbine initiates rotation at specific speeds dictated by the water's velocity. This rotational movement of the water wheel generates both mechanical and electrical power concurrently. The float method in Fig. 4 is applied to determine the water velocity and will be further discuss in next section.

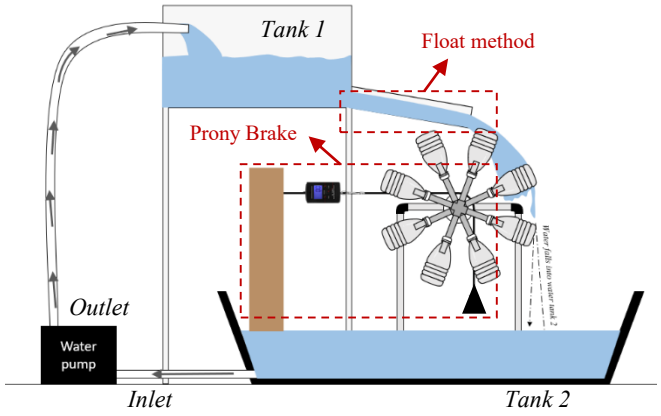

Fig. 4. Schematic of water test rig.

In a real-world application, water tank 1 is filled with river water, and the water is then directed back into the river after passing through the water wheel turbine.

4. Governing Equations

Before measuring the mechanical power generated, it's imperative to determine the force, F acting on the water wheel. Hence, a critical system known as the Prony brake is employed to measure this force [9, 30]. Fig. 5 illustrates the schematic of the Prony brake system used for force measurement.

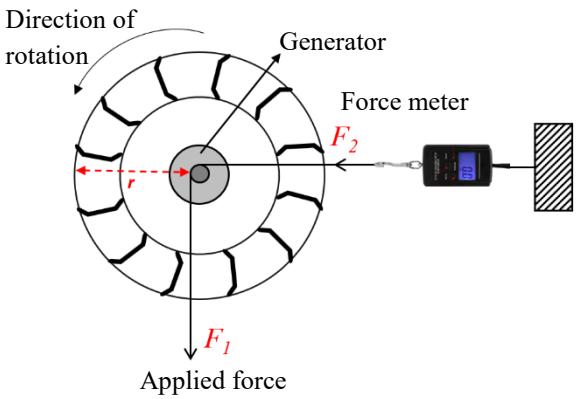

Fig. 5. Prony brake scheme.

The force, F (N) generated by the wheel is measured using Eq. (1).

$$F = F_2 - F_1 \quad (1)$$

where F_1 refers to the applied weight (N) that is employed to the device until the wheel stop rotates, while F_2 is the result

of the force meter (N). Then, the torque, τ (Nm) is calculated once the force, F is obtained using Eq.(2).

$$\tau = F\, r \tag{2}$$

where r is the radius of the pulley (m). Hence, the mechanical power, P_{mech} (W) of wheel can be obtained using Eq. (3).

$$P_{mech} = \tau\, \omega \tag{3}$$

Meanwhile, the angular velocity, ω (rad/s) can be determined using Eq. (4).

$$\omega = 2\pi\, n / 60 \tag{4}$$

where n refers to the rotational speed (rpm) of the wheel turbine that is measured using tachometer. Furthermore, the potential power, $P_{potential}$ (W) can be obtained through Eq. (5).

$$P_{potential} = \rho\, g\, Q\, H \tag{5}$$

where water flow rates, Q (m^3/s) is measured based on the volume of water passing through an area during a period of time.

Meanwhile, water head, H (m) is obtained using the Bernoulli equation. As for water density, ρ (kg/m^3) and gravity acceleration, g (m/s^2), both are fixed at $1000 kg/m^3$ and $9.81 m/s^2$. Hence, Eq. (6) was used to obtain the value of Q.

$$Q = v\, A \tag{6}$$

where v is water velocity and A (m^2) is the surface area of water in channel. Hence, A can be determined based on the parameters in Fig. 5, as in Eq. (7).

$$A = L\, T \tag{7}$$

Based on Fig. 6, both T (m) and L (m) refers to the height and width of water in channel. The channel functions as a penstock, serving to transport water from the water tank to the turbines. Meanwhile, the parameter H in the system is estimated using the Bernoulli equation, as outlined in Eq. (8), with the water velocity, v, being measured using the float method.

$$H = v^2 / 2g \tag{8}$$

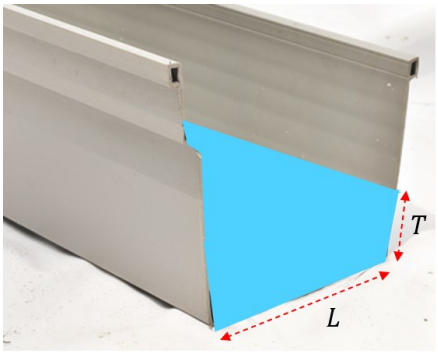

Fig. 6. Scheme of the parameters of the water in channel.

The water velocity, v (m/s) is determined by using float method as discussed by [24, 25]. During float method, a float object is passed the distance from the first measurement point to the second measurement point which denoted as ℓ (m). Then, the time taken, t (s) for the object to travel is recorded using a stopwatch. Thus, v can be obtained using the Eq. (9).

$$v = \ell / t \tag{9}$$

Next, the value of voltage, V (V) and current, I (A) are measured using the multimeter. Thus, Eq. 10 is used to calculate electrical power, P_{elec} (W) produced by the system.

$$P_{elec} = V\, I \tag{10}$$

Finally, the efficiencies of mechanical and electrical (%) were calculated using the Eq. (11) and Eq. (12).

$$\eta_{mech} = (P_{mech} / P_{potential})\ 100\% \tag{11}$$

$$\eta_{elec} = (P_{elec} / P_{potential})\ 100\% \tag{12}$$

5. Basic Parameters Measuring

In this water wheel experiment, there are three adjustable parameters. The first is the number of blades attached to the water wheel, the second is the level of water head applied for hydropower generation, and lastly the applied force exerted to Prony Brake. Additionally, the Prony Brake, as shown in Fig. 7, involves two types of forces: the applied force (F1) and the force meter (F2). F1 is generated by incrementally adding mass, such as small bricks, as detailed in Table 1, until the water wheel ceases its rotation. Meanwhile, F2 is determined from the reading on an electronic scale. Once the values of F1 and F2 are established, Equation 1 can be utilized to calculate the available force within the system (F).

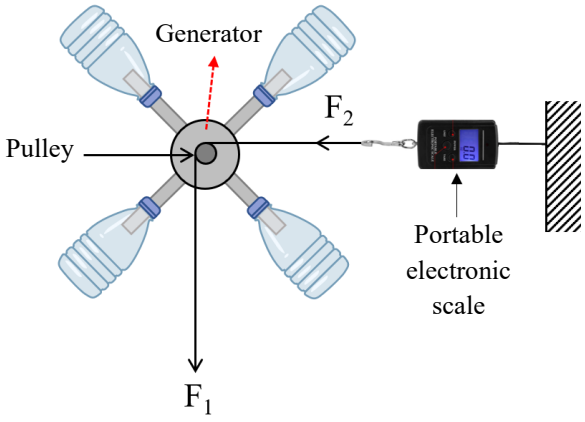

Fig. 7. Prony brake scheme on BOWW turbine.

A digital stopwatch is utilized to measure the time it takes for an object to travel a specified distance in the downstream channel. This time interval is crucial for determining the surface velocity of the water, v. In a schematic representation of the float method, as depicted in Fig. 8, the water's velocity can be calculated using Eq. (9), where the total length of the channel, ℓ is divided by the time taken, t for the object to cover the specified distance. Within this float method, an object is positioned on the surface of the flowing water in an open downstream channel.

This floating process is repeated multiple times to obtain an average value. Subsequently, the value of the water head

can be determined using Eq. (8), given that the water velocity has a significant impact on the water head.

Table 1. Variable parameters in the experimental work

Blades, B	Water head, H (m)	Applied force, F_1 (N)
8	0.3	0, 0.5, 1, 1.5, 2, 2.5, 3, 3.5, … until obtain the average value of F_1, increase with 0.5N.
	0.4	0, 0.5, 1, 1.5, 2, 2.5, 3, 3.5, … until obtain the average value of F_1, increase with 0.5N.
	0.5	0, 0.5, 1, 1.5, 2, 2.5, 3, 3.5, … until obtain the average value of F_1, increase with 0.5N.
4	0.3	0, 0.5, 1, 1.5, 2, 2.5, 3, 3.5, … until obtain the average value of F_1, increase with 0.5N.
	0.4	0, 0.5, 1, 1.5, 2, 2.5, 3, 3.5 … until obtain the average value of F_1, increase with 0.5N.
	0.5	0, 0.5, 1, 1.5, 2, 2.5, 3, 3.5 … until obtain the average value of F_1, increase with 0.5N.

A digital stopwatch is utilized to measure the time it takes for an object to travel a specified distance in the downstream channel. This time interval is crucial for determining the surface velocity of the water, v.

In a schematic representation of the float method, as depicted in Fig. 8, the water's velocity can be calculated using Eq. (9), where the total length of the channel, ℓ is divided by the time taken, t for the object to cover the specified distance. Within this float method, an object is positioned on the surface of the flowing water in an open downstream channel.

This floating process is repeated multiple times to obtain an average value. Subsequently, the value of the water head can be determined using Eq. (8), given that the water velocity has a significant impact on the water head.

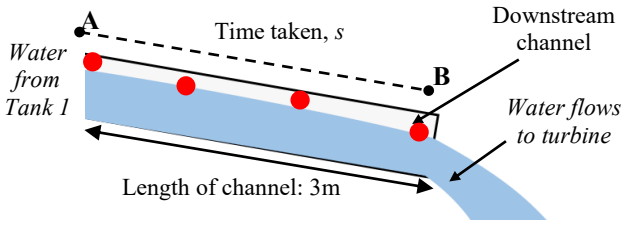

Fig. 8. Float method for measuring velocity and water head in the channel.

6. Results and Discussions

6.1 Potential Energy

The proposed overshot water turbine and pico-hydro system have been evaluated under conditions of extremely low head water which are 0.3m, 0.4m and 0.5m. The experiments were carried out to assess the performance of the proposed system. Furthermore, the experimental results are of utmost importance in identifying the key parameters that influence the system's performance.

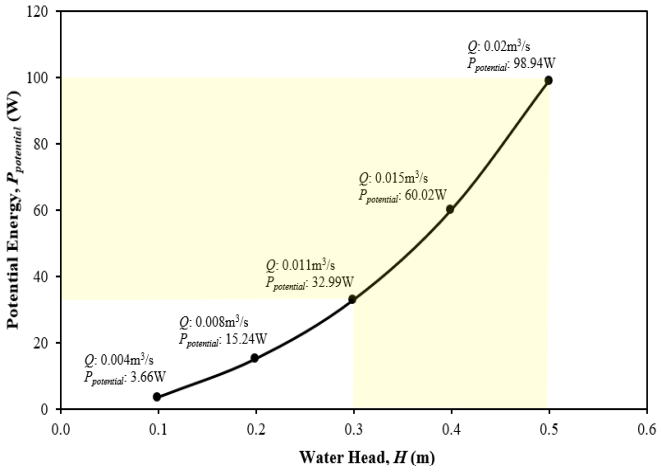

Fig. 9. Potential energy for various water head.

Fig. 9 shows the results of potential energy for various water head levels. Meanwhile, the shaded yellow region denotes the specific research areas, specifically at water head levels of 0.3m, 0.4m, and 0.5m. It can be deduced that the potential energy of the water wheel system exhibits a direct correlation with the water head level. This pattern aligns with the Eq. (5), highlighting the significant impact of water head on the potential power within the system.

Consequently, a higher water head level leads to an increased potential energy in the system [31]. The other significant parameter affecting the potential power is the water flow rate. İt varies according to specific water head conditions. The water velocity is the primary factor that affects both the water head and water flow rate, as stated in Eq. (6) and Eq. (8).

6.2 Force, Torque and Angular Velocity

The relationship between the parameters of force, torque and angular velocity is presented in Fig. 10 to Fig. 13. The experiments were carried out under three different levels of water head, which are 0.3m, 0.4m and 0.5m.

Both figures present the experimental results for eight and four numbers of blades attached to the system. Meanwhile, Table 1 presents a compilation of the maximum force and torque values achieved when operating with a 0.5m water head for both eight and four blades.

Table 2. Maximum values of force and torque at 0.5m head

	Eight blades	Four blades
Maximum Force	7.2N	4.64N
Maximum Torque	3.42Nm	2.2Nm

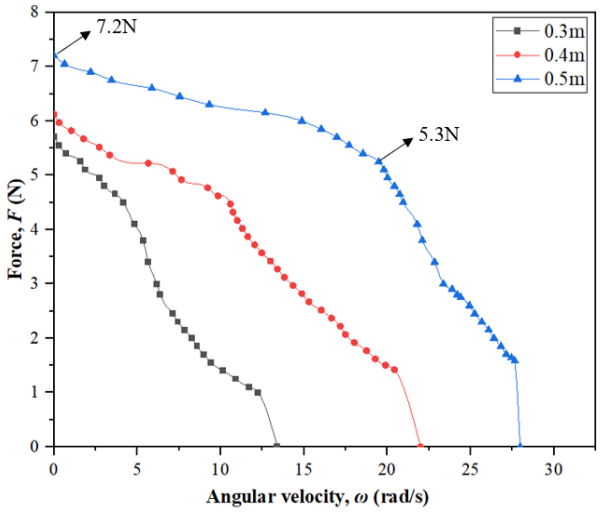

Fig. 10. Experimental force for water heads of 0.3m, 0.4m and 0.5m using eight blades.

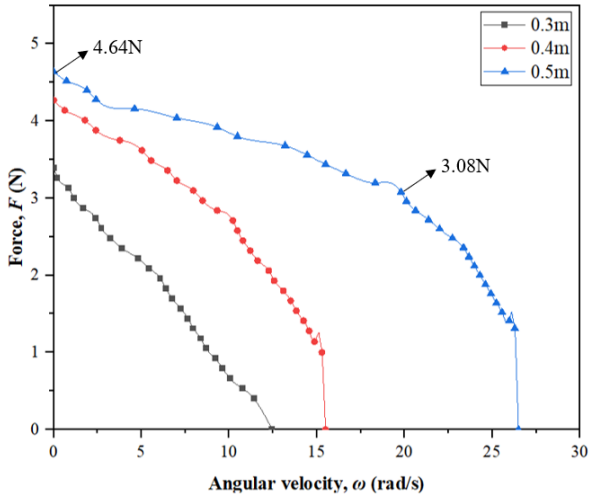

Fig. 11. Experimental force for water heads of 0.3m, 0.4m and 0.5m using four blades.

Before going through the discussion, it is essential to emphasize that the experimental work starts from the highest angular velocity and gradually decreases until the turbine eventually stops moving. In reference to Fig. 10 to Fig. 13, the peak values of force and torque were recorded at a 0.5m water head for both eight and four blades, respectively. Specifically, for eight blades, the maximum force reached 7.2N, while the maximum torque was measured at 3.42Nm. On the other hand, for four blades, the highest force recorded was 4.64N, with the maximum torque at 2.2Nm.

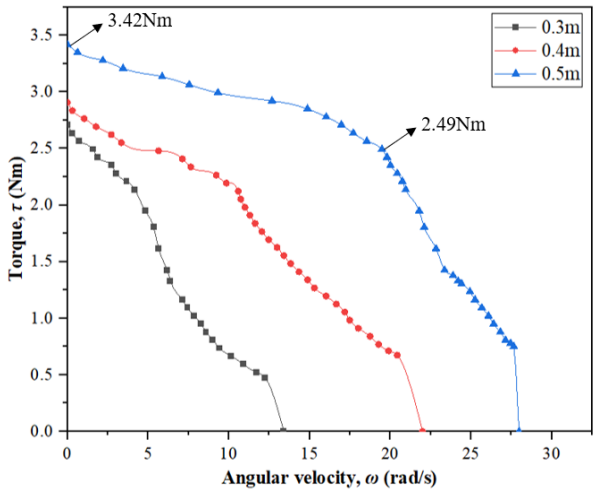

Fig. 12. Experimental torque for water heads of 0.3m, 0.4m and 0.5m using eight blades.

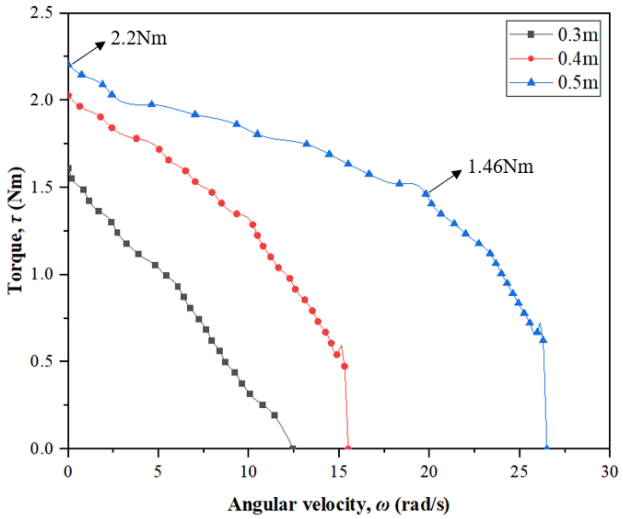

Fig. 13. Experimental torque for water heads of 0.3m, 0.4m and 0.5m using four blades.

Meanwhile, for four blades, the maximum force was determined to be 4.64N, and the maximum torque was measured at 2.2Nm. In general, it can be observed that the water head significantly influences the results of force and torque. As a result, the BOWW turbine is capable to generates higher force and torque when increases the water head. Besides that, the torque and force increase rapidly during high angular velocity. However, at a certain point, the rate of increase in torque and force slows down until it reaches their maximum value at zero angular velocity.

Furthermore, referring to Eq. (4), the angular velocity is determined by the rotational speed of turbine, which explains why the pattern of the values is similar to each other. This relationship is crucial in understanding the behavior of rotating turbines. When force is applied to the blades of a turbine, it generates torque as the blades rotate around the axis [32]. Furthermore, the force and torque are correlated, resulting in a comparable curve pattern, since torque is affected by the component of in Eq. (2). To clarify any change

in force directly influences the torque exerted by the turbine. Hence, an increase in force will lead to a corresponding increase in torque.

6.3 Mechanical Power

The relationship between two parameters, mechanical power and angular velocity is presented in Fig. 14 and Fig. 15. The experiments are conducted under three different levels of water head, which are 0.3m, 0.4m and 0.5m. Both figures shows the experimental results for eight and four numbers of blades.

In reference to Fig. 14 and Fig. 15, the BOWW turbine effectively converts potential energy into higher power output, especially when equipped with eight blades. This enhanced performance can be attributed to the fact that the BOWW turbine with eight blades generates greater force and velocity. These two key parameters, force and velocity, play a pivotal role in determining water head and flow rate, which, in turn, significantly influence potential power, as indicated in Eq. (5). Additionally, both key parameters are directly impact the energy transfer and the performance of the water wheel within a hydropower system [33]. Besides, mechanical power generated by the turbine increases towards the higher water head.

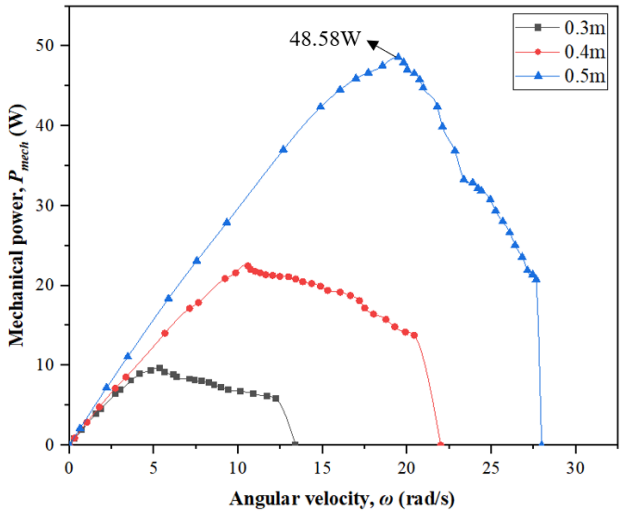

Fig. 14. Experimental mechanical power for water heads of 0.3m, 0.4m and 0.5m using eight blades.

Notably, there is a substantial contrast in the data for each water head level. For instance, the BOWW turbine operating at a 0.5m head with eight blades generated a maximum power output of 48.58W, while at a 0.4m head, it reached up to 22.46W. In contrast, the power generated at a 0.3m water head was notably lower at only 9.64W.

Conversely, when employing four blades, the BOWW turbine attained the highest power output of 25.33W at a 0.5m head and 13.15W at a 0.4m head. The minimum mechanical power generation, measuring only 5.66W, was observed at a water head of 0.3m. The angular velocity of the turbine played a substantial role in determining mechanical power, as it is the product of torque and rotational speed, as described in Eq. 3.

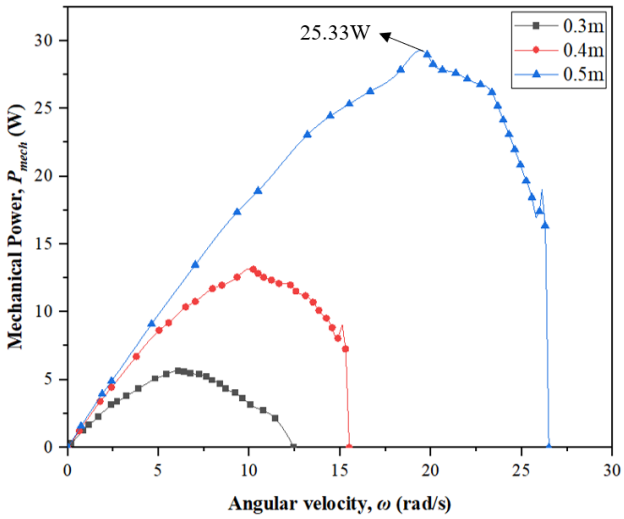

Fig. 15. Experimental mechanical power for water heads of 0.3m, 0.4m and 0.5m using four blades.

To summarize, the system exhibited its highest level of performance at a head of 0.5m, followed by the 0.4m head, whereas its efficiency was lowest at a head of 0.3m. Eq. (8) determines the operating water head, considering both the water velocity and gravitational acceleration. During the entire experiment, the value of gravitational acceleration remained consistent at 9.81m/s².

Meanwhile, water velocity varies depending on the time it takes for water to travel in the open channel, as indicated in Eq. (9). Therefore, water velocity also has an impact on the water flow rate and the dimensions of the channel, as detailed in Eq. (6). In simple terms, the behaviour of BOWW shows that an increase in water head results in a significant increase in water flow rate.

6.4 Electrical Power

Table 3 provides a summary of the electrical power tests conducted on the BOWW turbine equipped with eight bottle blades at a 0.5m water head. During the experiment, a load or force was incrementally applied to the Prony brake system with a consistent 0.5N increment. The electrical power generated for each load was measured to evaluate the system's performance in terms of electricity production.

The exact experimental procedures were employed for the BOWW turbines operating at different water head levels and with varying numbers of blades to ensure precise results. As a result, the amount of electrical power generated is so much less than mechanical energy generated due to the losses such as load and transmission losses that occur during the conversion process. However, these losses are ignored throughout the experiment.

Referring to Table 3, the electrical power gradually increases from 6.43W until it reaches its peak electrical power

output at 15.55W (highlighted in the blue box). This maximum power is achieved along with the highest electrical efficiency of 15.71% when the applied force ranges from 0 to 11N. Nevertheless, the electrical power experiences a decline, reaching a value of 15.21W when a force of 11.5N is applied. As for current and voltage, the table shows that the voltage increases while current decreases throughout the experiment in BOWW system. It can be seen that, the voltage increased to 39V when add force up to 11.5N, but more than 11.5N the resulting current is slightly reduced from 4A to 0.39A. Consequently, this reduction in current leads to a decrease in the electrical power generated.

Table 3. Electrical power test summary of eight blades BOWW turbine at 0.5m

Load no.	Applied force, F_1 (N)	Voltage, V (V)	Current, I (A)	Rotational speed, n (rpm)	Electrical power, P_{elec} (W)	Electrical efficiency, η_{elec} (%)
0	0	7.56	0.85	267	6.43	4.23
1	0.5	8.10	0.82	264	6.64	6.71
2	1	8.55	0.8	262	6.84	6.91
3	1.5	9.22	0.76	259	7.01	7.09
4	2	10.33	0.73	256	7.54	7.62
5	2.5	11.44	0.701	252	8.02	8.11
6	3	12.91	0.66	249	8.52	8.61
7	3.5	14.24	0.63	245	8.97	9.07
8	4	15.41	0.61	241	9.40	9.5
9	4.5	16.69	0.59	238	9.85	10
10	5	17.29	0.59	233	10.20	10.31
11	5.5	18.39	0.56	231	10.30	10.41
12	6	19.87	0.53	228	10.53	10.64
13	6.5	21.17	0.503	223	10.65	10.77
14	7	23.60	0.5	218	11.80	11.93
15	7.5	26.58	0.48	211	12.76	12.9
16	8	28.83	0.471	208	13.58	13.72
17	8.5	31.84	0.45	200	14.33	14.48
18	9	34.09	0.43	198	14.66	14.82
19	9.5	34.65	0.43	195	14.90	15.06
20	10	35.83	0.42	191	15.05	15.21
21	10.5	37.41	0.41	189	15.34	15.51
22	11	38.88	0.4	186	15.55	15.71
23	11.5	37.01	0.39	177	14.43	15.38

*** The blue box refers to the highest value of electrical power generated by the BOWW turbine with eight blades when operated at 0.5m of water head.*

6.5 Optimum Performance of BOWW

According to Table 4, the turbine achieves its best efficiency when running with a water head of 0.5m, regardless of whether it has eight or four blades. The efficiency levels are 49% for eight blades and 29.27% for four blades. The turbine with eight blades stands out as the most efficient among all the conditions, achieving a remarkable performance of 49.1% efficiency at a 0.5m water head. At a rotating speed beyond 186rpm, the BOWW turbine has the capacity to produce a maximum power output of 48.58W. Conversely, the turbine with four blades generates a maximum mechanical power of around 28.96W when it rotates at a speed of 165rpm.

According to the optimal value in Table 4, it is evident that the water flow rate is identical for both quantities of blades. This is due to the association between the water head and flow rate, which is caused by the velocity of water flowing in the channel during the experimental process.

6.6 Comparison with Previous Studies

The parameter U/v on the x-axis represents the ratio of the tangential velocity of the turbine to the velocity of the water. The tangential velocity of the turbine, U corresponds to the linear speed of the turbine while it rotates. As per Ramdhani [23], U is a crucial parameter that notably impacts the performance of the water wheel. Nevertheless, U is largely

dependent on the rotational speed, n and the diameter of the turbine, D, as demonstrated in Eq. (13) below.

$$U = (n / 60)\, D \quad (13)$$

In Fig. 16 and Fig. 17, the BOWW equipped with eight blades achieved exceeding 49% of mechanical efficiency, surpassing the breastshot water wheel by Sari [26] with a mechanical efficiency of about 45% and BOWW with four blades that achieved 29% of mechanical efficiency. In terms of electrical efficiency, the BOWW with eight blades reached around 24% efficiency, followed by the BOWW with four blades at 11%.

Table 4. Optimum value recorded when equipped with different number of blades

Blades	H (m)	Q (m^3/s)	n (rpm)	ω (rad/s)	P_{mech} (W)	η_{mech} (%)	P_{elec} (W)	η_{elec} (%)
8	0.5	0.021	186	19.48	48.58	49.1	15.55	15.71
	0.4	0.016	101	10.58	22.46	37.44	7.18	11.98
	0.3	0.012	51	5.34	9.64	26.8	5.61	6.21
4	0.5	0.021	165	17.28	28.96	29.27	9.26	9.4
	0.4	0.016	97	10.21	13.15	21.91	4.2	7
	0.3	0.012	58	6.08	5.66	17.72	1.3	3.2

The breastshot water wheel, on the other hand, achieved only 4.6% electrical efficiency. It's worth noting that the authors of undershot and overshot water wheel types did not provide electrical efficiency measurements, making a direct comparison impossible. The breastshot water wheel consisted of sixteen steel blades and operated at a 0.26m water head with a water flow rate of 0.09708m^3/s. At the conclusion of the experiment, it was observed that the breastshot water wheel failed to attain optimal efficiency at water flow rates below 0.1m^3/s and water heads less than 1m.

In contrast, the overshot water wheel demonstrated a mechanical efficiency that was 59% superior to that of the BOWW. It is essential to note that the BOWW turbine required an extremely low water head of 0.5m with a constant flow rate of 0.0201m^3/s, whereas the overshot water wheel necessitated a 1m water head and varying flow rates between 0.005m^3/s and 0.013m^3/s.

All water wheels, including the BOWW, generally exhibit a similar curve pattern of behavior. However, the experimental data for the overshot water wheel in Fig. 18 terminates at its highest point. This is because the system failed to operate at rotational speeds below 15rpm, equivalent to 0.225 U/v [26].

Additionally, all water wheels initially remain in a static state (with no force acting against the wheel) until the flowing water strikes the blades, initiating rotational movement. Simultaneously, the resulting force gradually increases, leading to a gradual decrease in the rotational speed of the water wheel until it eventually stops rotating after reaching the maximum force (the force is determined using the Prony Brake scheme, as discussed earlier).

Theoritically, it can be concluded that parameters such as rotational speed, n and force, F significantly influence mechanical efficiency, which is related to the parameter P_{mech}. On the other hand, parameters such as voltage (V) and current (I) determine the value of electrical efficiency, represented by P_{elec}.

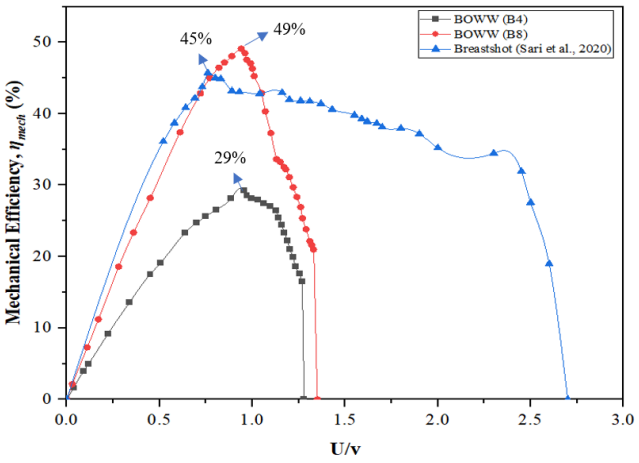

Fig. 16. Mechanical efficiency curves for BOWW four blades, BOWW eight blades and breastshot water wheel.

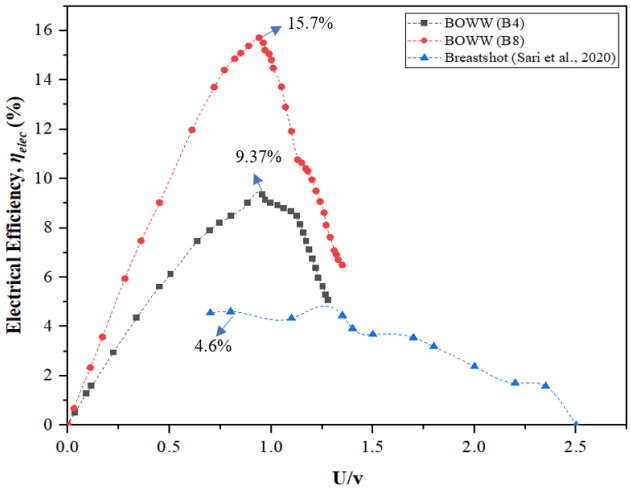

Fig. 17. Electrical efficiency curves for BOWW four blades, BOWW eight blades and breastshot water wheel.

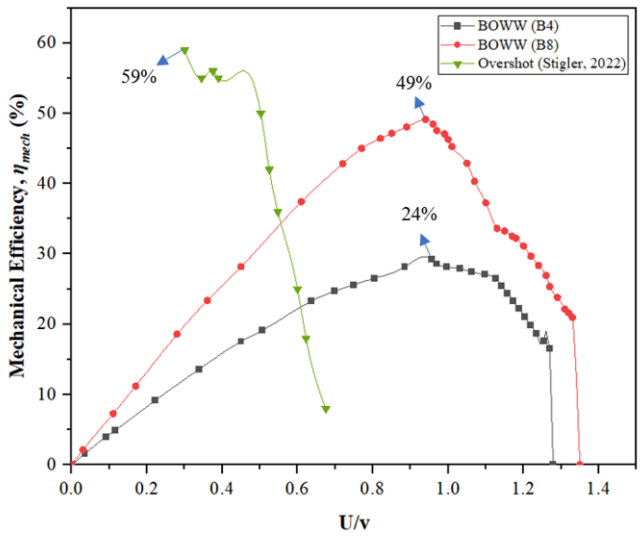

Fig. 18. Mechanical efficiency curves for BOWW four blades, BOWW eight blades and overshot water wheel.

Therefore, higher values of P_{mech} and P_{elec} correspond to higher values of η_{mech} and η_{elec}. Additionally, it is observed that the efficiencies of these water wheels converge as U/v approaches zero but diverge at higher U/v values. This divergence occurs because each water wheel rotates at different speeds and eventually stops when it can no longer accommodate the maximum force.

7. Conclusion

The performance of the bottle blade overshot water wheel was evaluated, and several findings were discussed in this paper. This project involved the replacement of the conventional design of overshot water wheel blades with polythene bottle or plastic soda bottles. Furhermore, this innovative blade design makes use of standard PVC pipe connections that are readily available and easily adjustable. In essence, this turbine can be operated by anyone with a rudimentary understanding of pipes.

It is crucial to emphasize that the BOWW turbine consistently delivered good performance during the experimental work, particularly under low water head and low flow rate operating conditions. This is based on the experimental results, which demonstrated the capabilities of the BOWW turbine, particularly when equipped with eight blades and operates at a 0.5m water head. The BOWW with eight blades demonstrated a good mechanical efficiency up to 49% and an electrical efficiency around 15.55%.

Therefore, it can be concluded that the BOWW turbine meet the expectations outlined in the hypothesis, particularly in terms of its performance under specified conditions, in less than 0.5m water head. Besides, this low cost BOWW turbine is expected to generate sufficient amount of electricity around 120kW per year to power up electrical appliances such as lighting for a small farm or any suitable places in rural areas.

The blade design which makes use of plastic soda bottles, and the incorporation of readily available PVC pipe connections demonstrate a unique and practical approach to turbine construction. This design choice not only demonstrates creativity but also addresses practical considerations, contributing to the turbine's overall ease of operation. This emphasis on simplicity and accessibility highlight the turbine's potential for widespread use. Its straightforward design and the use of commonly available materials contribute to its adaptability in diverse settings. Whether in remote areas or regions with limited resources, the turbine's construction and operation are feasible, promoting its potential for widespread adoption.

In some cases, the turbine's simplicity and the use of readily available materials make it suitable for emergency power generation. The BOWW turbine could offer a prompt and easily accessible method of producing electricity in areas affected by disasters or in temporary installations. Besides, it also holds the potential for community-based projects especially in off-grid areas. Local communities could collaboratively build and maintain these turbines, fostering a sense of ownership and sustainability.

In conclusion, the BOWW turbine, with its innovative blade design using plastic soda bottles and the use of readily available PVC pipe connections, presents a paradigm shift in the realm of small-scale hydropower. The demonstrated high efficiency, particularly under challenging conditions, not only propels the turbine as a viable and sustainable energy solution but also underscores its potential for diverse applications, ranging from off-grid communities to educational initiatives. This research not only enhances the progress of renewable energy technologies but also promotes the principles of simplicity, accessibility, and community empowerment.

Acknowledgements

This research project was supported by the Ministry of Higher Education (MOHE) Malaysia through the Fundamental Research Grant Scheme (FRGS) (Grant No. FRGS/1/2024/TK08/UTEM/02/6). The authors gratefully acknowledge Universiti Teknikal Malaysia Melaka (UTeM) for the facilities and support provided.

References

[1] T. S. Kishore, E. R. Patro, V. S. K. V. Harish, and A. T. Haghighi, “A comprehensive study on the recent progress and trends in development of small hydropower projects,” Energies. 2021.

[2] M. Basar, N. Mohd Rais, A. Rahman, W. Mustafa, K. Sopian, and K. Wong, “Optimization of Reaction Typed Water Turbine in Very Low Head Water Resources for Pico Hydro,” J. Adv. Res. Fluid Mech. Therm. Sci., vol. 90, pp. 23–39, Dec. 2021.

[3] N. A. M. Rais, M. F. Basar, S. F. A. Gani, and W. A. Mustafa, “Techno-Economic Evaluations: An Innovative of Hydraulic Reaction Turbine for Pico-Hydro Generation System,” J. Adv. Res. Fluid Mech. Therm. Sci., vol. 90, no. 2, 2022.

[4] A. O. Egorov, M. A. Sadokhina, D. E. Petrushin, and Y. I. Sysoeva, "The Overview of the Park of Hydro Turbines of Mini-Hydro Power Plants in Russia," in 2022 Conference of Russian Young Researchers in Electrical and Electronic Engineering (ElConRus), 2022, pp. 608–612.

[5] S. Tang, J. Chen, P. Sun, Y. Li, P. Yu, and E. Chen, "Current and future hydropower development in Southeast Asia countries (Malaysia, Indonesia, Thailand and Myanmar)," Energy Policy, 2019.

[6] S. Salim and A. I. Tolago, "Use of Coconut Shell Become an Alternative Electricity," Int. J. Smart grid, vol. 7, no. V7i3, 2023.

[7] N. A. Mohd Rais and M. F. Basar, "Parametric analysis on a simple design water reaction turbine for low-head low-flow Pico-hydro generation system," J. Mech. Eng. Sci., vol. 15, no. 3, 2021.

[8] J. A. Hameed, A. T. Saeed, and M. H. Rajab, "Design and Study of Hydroelectric Power Plant by Using Overshot and Undershot Waterwheels," Int. J. Energy Optim. Eng., 2019.

[9] M. F. Basar, I. A. Zulkarnain, A. A. Rahman, and K. Sopian, "An Experimental Investigation of Overshot Waterwheel in Very Low Head Water Resources for Pico Hydro," Int. J. Eng. Appl. (IREA); Vol 10, No 3, May 2022.

[10] Budiarso, D. Adanta, Warjito, A. I. Siswantara, P. Saputra, and R. Dianofitra, "Optimization of the Water Volume in the Buckets of Pico Hydro Overshot Waterwheel by Analytical Method," in IOP Conference Series: Materials Science and Engineering, 2018.

[11] E. Quaranta and R. Revelli, "Gravity water wheels as a micro hydropower energy source: A review based on historic data, design methods, efficiencies and modern optimizations," Renewable and Sustainable Energy Reviews. 2018.

[12] E. Y. Setyawan, S. Djiwo, D. H. Praswanto, P. Suwandono, and P. Siagian, "Design of Low Flow Undershot Type Water Turbine," J. Sci. Appl. Eng., vol. 2, no. 2, 2019.

[13] A. Fernando, A. Tesalona, E. Fuentebella, F. Franco, C. Chua, I. Aquino, R.R. Vicerra, "Simulation of a Rain-Powered Pico-Hydro Generator for a House Application," in 2021 IEEE 13th International Conference on Humanoid, Nanotechnology, Information Technology, Communication and Control, Environment, and Management (HNICEM), 2021, pp. 1–4.

[14] V. Z. Delante, V. J. Ylaya, R. R. P. Vicerra, and R. R. Bacarro, "Energy Potential of Macopa Irrigation using Pico-Hydro Power Plant Design Utilizing Under-Shot Type Waterwheel," in 2021 IEEE 13th International Conference on Humanoid, Nanotechnology, Information Technology, Communication and Control, Environment, and Management (HNICEM), 2021, pp. 1–6.

[15] A. Bachan, N. Ghimire, J. Eisner, S. Chitrakar, and H. Prasad Neopane, "Numerical analysis of low-tech overshot water wheel for off grid purpose," in Journal of Physics: Conference Series, 2019.

[16] M. Yaakub, M. Başar, F. Hanim, and H. Boejang, "Pico-hydro Electrification from Rainwater's Gravitational Force for Urban Area," Telkomnika (Telecommunication Comput. Electron. Control., vol. 16, pp. 997–1003, Jun. 2018.

[17] M. N. Hidayat, I. H. Eryk, M. F. Hakim, F. Ronilaya, S. Wibowo, and S. Syahroni, "Utilization of the Overshot Waterwheel at the Pico Hydro Power Generation for Electrification of Remote Areas," in Proceedings - IEIT 2021: 1st International Conference on Electrical and Information Technology, 2021.

[18] K. P. Moe, E. E. MYAT, C. C. KHAING, and Z. M. NWE, "Design of 10 kW Water Wheel for Micro-Hydro Power," Int. J. Sci. Eng. Technol. Res., 2019.

[19] T. Venkata, S. Kalyani, K. Venkata, G. Rao, and G. Sanjeev, "Amalgamation of Smart Grid with Renewable Energy Sources," Int. J. Smart grid, vol. 7, no. V7i2, 2023.

[20] A. YoosefDoost and W. D. Lubitz, "Archimedes screw turbines: A sustainable development solution for green and renewable energy generation-a review of potential and design procedures," Sustain., 2020.

[21] L. Sule, A. A. Mochtar, and O. Sutresman, "Performance of undershot water wheel with bowl-shaped blades model," Int. J. Technol., 2020.

[22] A. M. A. Morris, "John smeaton and the vis viva controversy: Measuring waterwheel efficiency and the influence of industry on practical mechanics in britain 1759-1808," Hist. Sci., 2018.

[23] M. R. Ramdhani, R. Irwansyah, Budiarso, Warjito, and D. Adanta, "Investigation of the 16 blades pico scale breastshot waterwheel performance in actual river condition," J. Adv. Res. Fluid Mech. Therm. Sci., 2020.

[24] Budiarso, Warjito, M. Naufal Lubis, and D. Adanta, "Performance of a low cost spoon-based turgo turbine for pico hydro installation," in Energy Procedia, 2019, vol. 156.

[25] A. Chamas, H. Moon, J. Zheng, Y. Qiu, T. Tabassum, J. H. Jang, M. A. Oman, S. L. Scott, S. Suh, "Degradation Rates of Plastics in the Environment," ACS Sustain. Chem. Eng., vol. 8, no. 9, 2020.

[26] D. P. Sari, Helmizar, I. Syofii, Darlius, and D. Adanta, "The effect of the ratio of wheel tangential velocity and upstream water velocity on the performance of undershot waterwheels," J. Adv. Res. Fluid Mech. Therm. Sci., vol. 65, no. 2, 2020.

[27] Budiarso, Helmizar, Warjito, A. Nuramal, W. Ramadhanu, and D. Adanta, "Performance of breastshot waterwheel in run of river conditions," in AIP Conference Proceedings, 2020.

[28] J. Štigler, "Overshot water wheel efficiency measurements for low heads and low flowrates," EPJ Web Conf., vol. 269, p. 1058, Oct. 2022.

[29] A. Ramadhan and Asral, "Design and performance test of overshot water wheel with variation of inner diameter," J. Tek. Mesin Indones., vol. 17, pp. 93–96, Oct. 2022.

[30] X. Shi, "The hydraulic tilt hammer in ancient China," in History of Mechanism and Machine Science, vol. 37, 2019.

[31] Z. Zou, L. Chen, H. Li, and X. Peng, "A Multi State Analysis for Small Hydropower Cluster," in 2022 4th International Conference on Intelligent Control, Measurement and Signal Processing (ICMSP), 2022, pp. 644–647.

[32] Pribadyo, Pribadyo, H. Hadiyanto, and J. Jamari, "Study of low head turbine propellers axial flow for use of micro-hydropower plant (MHP) in Aceh, Indonesia," in Journal of Physics: Conference Series, 2020.

[33] L. N. Mbele and K. Kusakana, "Model-Based Design of a Conduit Pico Hydropower System," in 2018 IEEE PES/IAS PowerAfrica, 2018, pp. 769–774.